

Functional ablation of the mouse *Ldb1* gene results in severe patterning defects during gastrulation

Mahua Mukhopadhyay^{1,*}, Andreas Teufel^{1,*}, Tsuyoshi Yamashita^{1,*†}, Alan D. Agulnick^{1,‡}, Lan Chen¹, Karen M. Downs², Alice Schindler¹, Alexander Grinberg¹, Sing-Ping Huang¹, David Dorward³ and Heiner Westphal^{1,§}

¹Laboratory of Mammalian Genes and Development, National Institute of Child Health and Human Development, National Institutes of Health, Bethesda, Maryland 20892, USA

²Department of Anatomy, University of Wisconsin-Madison Medical School, Madison, WI 53706, USA

³National Institutes of Allergy and Infectious Diseases, Rocky Mountain Laboratories, Hamilton, Montana 59840, USA

*These authors contributed equally to this work

†Present address: Department of Obstetrics and Gynecology, Asahikawa Medical College, Nishikagura 4-5-3-11, Asahikawa, Japan

‡Present address: CyThera Inc., 3550 General Atomics Court, San Diego, CA 92121, USA

§Author for correspondence (e-mail: hw@helix.nih.gov)

Accepted 18 October 2002

SUMMARY

The LIM domain-binding protein 1 (*Ldb1*) is found in multi-protein complexes containing various combinations of LIM-homeodomain, LIM-only, bHLH, GATA and Otx transcription factors. These proteins exert key functions during embryogenesis. Here we show that targeted deletion of the *Ldb1* gene in mice results in a pleiotropic phenotype. There is no heart anlage and head structures are truncated anterior to the hindbrain. In about 40% of the mutants, posterior axis duplication is observed. There are also severe defects in mesoderm-derived extraembryonic structures,

including the allantois, blood islands of the yolk sack, primordial germ cells and the amnion. Abnormal organizer gene expression during gastrulation may account for the observed axis defects in *Ldb1* mutant embryos. The expression of several Wnt inhibitors is curtailed in the mutant, suggesting that Wnt pathways may be involved in axial patterning regulated by *Ldb1*.

Key words: *Ldb1*, Wnt inhibitor(s), *Otx2*, Mouse, Anterior-posterior axis

INTRODUCTION

Ldb1 (also called NL1 or Clim-2), a LIM domain-binding protein, was isolated based on its ability to bind LIM domains present in LIM-homeodomain (HD) and LIM-only proteins (Agulnick et al., 1996; Jurata et al., 1996; Bach et al., 1997). *Ldb1* is thought to mediate transcriptional regulation by protein complexes consisting of LIM-HD and other classes of transcription factors such as GATA, bHLH and Otx (Agulnick et al., 1996; Jurata et al., 1996; Bach et al., 1997; Jurata and Gill, 1997; Visvader et al., 1997; Wadman et al., 1997; Breen et al., 1998; Dawid et al., 1998; Jurata and Gill, 1998). The protein-protein interactions with *Ldb1* may not be restricted to proteins containing LIM domains since Chip, the *Drosophila* homolog of *Ldb1*, also interacts with homeodomain proteins lacking LIM domains. A separate domain of Chip that is distinct from the LIM-binding domain appears to be involved in this interaction with other homeodomain proteins (Torigoi et al., 2000).

Genes homologous to *Ldb1* have been found in organisms as diverse as *C. elegans* and humans. While there are two distinct *Ldb* gene family members in vertebrates and four in zebrafish, only one member has been identified in *C. elegans* and *D. melanogaster* (Cassata et al., 2000). Gene duplication

events are thought to be responsible for the increase in the number of both the transcription factors and interacting *Ldb* proteins during the course of evolution (Meyer and Schartl, 1999).

LIM domains, cysteine-rich motifs that bind zinc and mediate protein-protein interactions, are found in many proteins expressed in the embryo (reviewed by Bach, 2000; Dawid et al., 1998). The biological consequences of disruption of LIM-HD transcription factors are severe, demonstrating the importance of these genes in development (for review, see Hobert and Westphal, 2000). It is well established that LIM domains have a negative regulatory effect on the function of LIM-homeodomain proteins (German et al., 1992; Taira et al., 1994; Sanchez-Garcia and Rabbitts, 1994). Embryo microinjection studies in *Xenopus* have shown that interactions between LIM domains and *Ldb1* help relieve the inhibitory effect of the LIM domains (Agulnick et al., 1996). The LIM-binding portion of *Ldb1* has been localized to the carboxyl terminus, while the amino-terminal region is involved in homodimer formation (Breen et al., 1998). The later domain may also allow formation of heterodimers with *Ldb2* (also called NL2 or Clim-1), the second member of the vertebrate *Ldb* family (Agulnick et al., 1996; Jurata et al., 1996; Bach et al., 1997).

The ubiquitous expression pattern of *Ldb1* during development and its interaction with numerous transcriptional regulators (Agulnick et al., 1996; Jurata et al., 1996; Bach et al., 1997; Jurata and Gill, 1997; Visvader et al., 1997; Wadman et al., 1997; Breen et al., 1998; Dawid et al., 1998; Jurata and Gill, 1998) suggest a critical function of the gene in a variety of developmental pathways. In order to provide direct genetic evidence for the role of mammalian *Ldb1* in embryonic development, we have eliminated its function in mice. *Ldb1* null mutants show severe anterior-posterior patterning defects that include anterior truncation, posterior duplication, and lack of heart and foregut formation. Functional impediments of the organizer genes *Otx2*, *Lim1* (*Lhx2*), *Dkk1*, *Hesx1* and *Hnf3 β* during gastrulation may account for the anterior-posterior axis patterning defect observed in the mutant at post-gastrulation stages of development. Our results suggest that defects in the regulation of Wnt pathways may be the underlying cause for the observed mutant phenotype.

MATERIALS AND METHODS

Generation of *Ldb1*^{-/-} mutant mice

Ldb1 genomic clones were isolated from a mouse 129/Sv genomic library (a gift from Dr S. Tonegawa, Massachusetts Institute of Technology, Cambridge, MA). The targeting vector was constructed by replacing exon 3-9 of *Ldb1* with a PGK-NEO cassette, preserving 4.3 kb (5') and 2.4 kb (3') of flanking homologous sequences and using the thymidine kinase gene for double selection. The final targeting vector was linearized at a unique *NotI* site before transfection of ES cells. Transfected ES cells were subjected to double selection. Targeted disruption of the *Ldb1* gene via homologous recombination was confirmed by Southern blot analysis. Genomic DNA isolated from ES cells was digested with *EcoRV* or *HindIII* for Southern analysis. A 0.3 kb *EcoRV*-*BglIII* fragment was used as a 5' probe to identify a 6.2 kb fragment of the mutated allele. A 0.45 kb *NcoI*-*NcoI* fragment served as the 3' probe to detect a 6.6 kb fragment of the mutated allele. Recombinant ES cells were injected into blastocysts to generate chimeric mice. Chimeric males were mated with C57BL/6 females to produce *Ldb1*^{+/-} animals, which were intercrossed to produce *Ldb1*^{-/-} offspring for analysis.

Genotyping

For genotypic analysis of E7.5 to E8.5 embryos, whole embryos were digested overnight upon completion of in situ analysis and photogramming. The genotype of the embryos was determined by polymerase chain reaction using the following primers: *Ldb1* wild-type allele primers 5'-CCATTGGCCGGACCCCTGATACCA-3' and 5'-CTGGGTAAACATGGGTTTGCCGTGCA-3'; NEO primers 5'-CTGGGTGGAGAGGCTATTC-3' and 5'AGGTGAGATGACAGG-AGATC-3', which yielded bands of 175 and 280 bp, respectively.

Detection of maternal *Ldb1* mRNA in oocytes

Total RNA from unfertilized eggs was isolated using Picopure RNA isolation kit from Arcturus (Cat. no. KIT0202). RNA quantification was performed using RiboGreen RNA Quantification Reagent and a kit from Molecular Probes (Cat. nos. R-11491 and R-11490). About 15 ng of RNA was used for RT-PCR analysis. RT-PCR was performed using Smart Race cDNA Amplification kit from Clontech. *Ldb1* primers used for RT-PCR analyses were as follows. Left primer 5'-GACAATCTCTGGTGGGATGCTTTCACAAC-3', right primer 5'-CATAAGTTCCTGCATGGCTCTAGTACTA-3'. Nucleotide sequences of the control primer set: left primer 5'-GAACAAG-

TACCAGACTCTTGACAAC-3', right primer 5'-GTTTACAGATCTTGGACCAGAAGTGTCT 3'.

Histology and in situ hybridization

For histological analyses, embryos were fixed in 4% paraformaldehyde, dehydrated, embedded in paraffin, sectioned at 5 μ m and stained with Hematoxylin and Eosin. In situ hybridization to whole embryos was performed as described previously (Saga et al., 1996) using antisense riboprobes to *Hesx1/Rpx* (Thomas and Beddington, 1996; Hermesz et al., 1996), *Otx2* (Simeone et al., 1993), *Brachyury* (*T*) (Herrmann, 1992), *Six3* (Oliver et al., 1995), *Hnf3 β* (Ang and Rossant, 1994), *Dkk1* (Glinka et al., 1998), *Wnt3* (Liu et al., 1999), *Wnt3a* (Takada et al., 1994), *Wnt8* (Bouillet et al., 1996), *Frzb* (Leyns et al., 1997; Hoang et al., 1998), *Sfrp1* (Hoang et al., 1998), *Sfrp2* (Leimeister et al., 1998) and *Cer1* (Belo et al., 1997).

Scanning electron microscopy

Dissected embryos were placed into Teflon baskets (Ted Pella, Redding, CA) and prepared for scanning electron microscopy by standard procedures. electron micrographs were taken at 10 kV on a Hitachi S4500 scanning electron microscope (Robards and Wilson, 1993).

Detection of blood islands

Embryos were fixed in 4% paraformaldehyde and washed in PBS. Staining of the blood islands was performed in a 0.1% benzidine solution dissolved in PBS and 0.1% glacial acetic acid.

Detection of primordial germ cells

Embryos were fixed in 4% paraformaldehyde and washed in PBS, 70% ethanol and H₂O. Primordial germ cells were stained in 5% veronal buffer, 0.6% MgCl₂, 0.1% α -naphthylphosphate and 0.5% Nuclear Fast Red.

RESULTS

Generation of *Ldb1* null mutant mice

Mice carrying a null allele of *Ldb1* were generated through homologous recombination in ES cells. The genomic organization of the *Ldb1* gene (Yamashita et al., 1998) and the vector used for gene targeting are shown in Fig. 1A. The targeting vector contained the neomycin-resistant gene, which replaced the coding region from exon 3 to exon 9 following homologous recombination. Two independent positive clones (Fig. 1B) were injected into C57BL/6 blastocysts to generate chimeric animals. Chimeric mice were crossed with CD1 females to obtain heterozygous offspring. Mice heterozygous for the *Ldb1* mutation appeared normal and fertile. Heterozygous mice were intercrossed to obtain homozygous mutants. No viable mutants were found at birth ($n=143$), or at E16.5 ($n=37$). Homozygous mutants died at E9.5-E10.

Ldb1 null mutant phenotype: defects in embryonic development

Functional ablation of the *Ldb1* gene led to a multitude of developmental defects along the anterior-posterior axis of the early mouse embryo. In comparison with wild-type (Fig. 2A), gastrulating mutant embryos showed a characteristic constriction at the embryonic-extraembryonic junction (Fig. 2B). The embryonic portion is generally smaller than that in the wild type. Mutant phenotypes were clearly visible at E8.5 and included anterior truncation, absence of heart formation

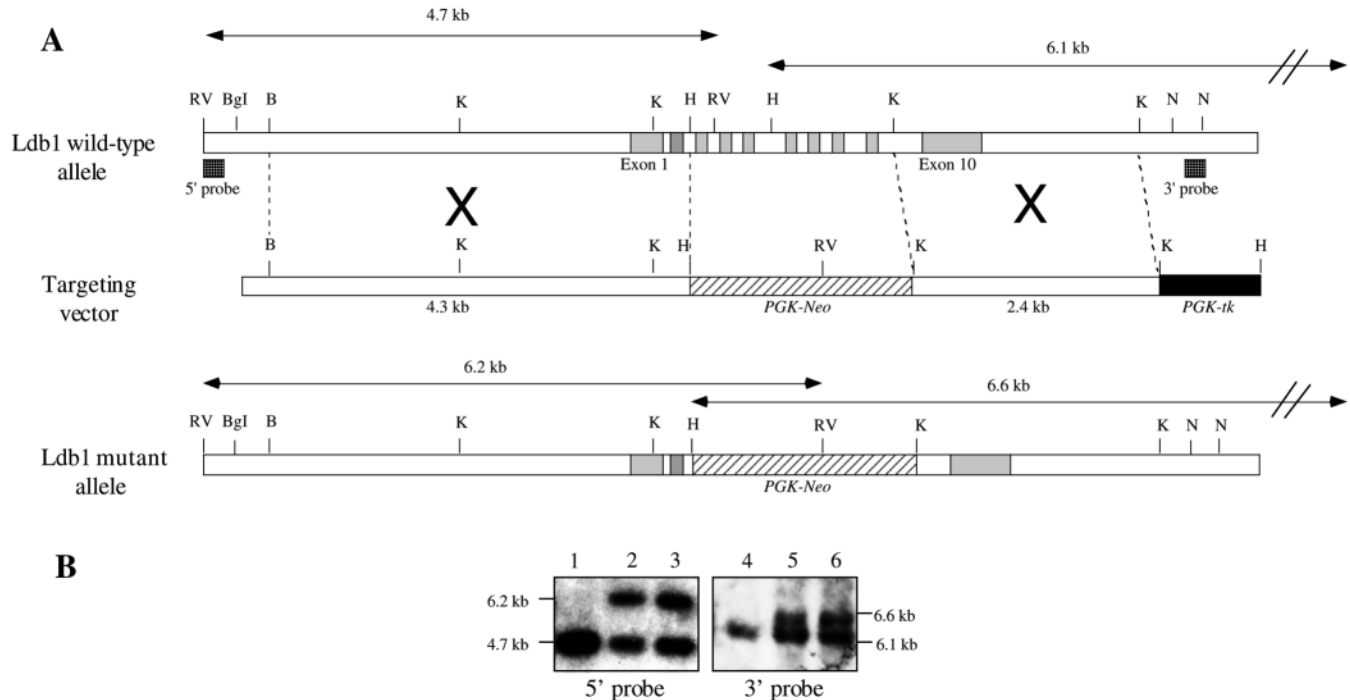


Fig. 1. Gene targeting at the *Ldb1* locus. (A), Partial restriction map of the wild-type *Ldb1* locus, the targeting vector, and disrupted *Ldb1* allele. A gene conferring neomycin-resistance replaces the deleted *Ldb1* coding sequences (exons 3-9) following homologous recombination. (B) Southern blot analysis of targeted ES cells. Two independent clones TS17 (lanes 2, 5) and TS153 (lanes 3, 6) were used for blastocyst injection. TS12 is a wild-type control (lanes 1, 4). *EcoRV*- and *HindIII*-digested ES cell DNA was used for Southern analyses with 5' and 3' probes respectively. The 5' probe hybridized to 4.7 kb and 6.2 kb restriction fragments generated from the wild-type and the mutated alleles respectively, while the 3' probe detected a 6.1 kb wild-type and a 6.6 kb mutant fragment.

and loss of foregut indentation (Fig. 2E, compared with the controls shown in Fig. 2C,D). *En2* expression that marks the midbrain-hindbrain boundary of wild-type embryos (Fig. 2F) is absent in the mutant (Fig. 2G,H) suggesting a disruption in midbrain and anterior hindbrain development. Also, the region of expression of *Krox20*, a hindbrain marker that marks rhombomeres r3 and r5 in the control (Fig. 2I), is abnormal in *Ldb1* mutant embryos (Fig. 2J). The pattern of head truncation in *Ldb1* mutant embryos was similar to that seen in the most severely affected *Otx2* mutants (Acampora et al., 1995; Ang et al., 1996). However, in contrast to *Otx2* mutants, the anterior region terminated in a convoluted neural plate structure implying a defect in the regional expansion of the neuroepithelium (Fig. 2L). *Ldb1* mutants lack all rostral structures anterior of the otic vesicle (Fig. 2L). Columns of somites were often fused medially. Defective longitudinal extension of the neuroepithelium is the likely cause of the kinky and compressed shape of the neural tubes in the mutant embryos. Histological sections of E8.5 mutants at the trunk level show two neural grooves that are connected by a single neuroepithelial layer (Fig. 2M). A similar phenotype has previously been observed in *Lim1* mutants (Shawlot and Behringer, 1995). Moreover, trunk duplication was observed visually in approximately 40% (24/56) of mutant embryos. Light and scanning electron microscopy revealed the presence of multiple rows of somites (Fig. 2N,O). The partial duplication of the *Krox2* signal (Fig. 2J) suggests that posterior axis duplication extends to the rostral limit of mutant embryos. Although *Ldb1* mutant embryos survived through stage E9.5,

further development appeared to be arrested at E8.5. This may be a consequence of an extensive apoptotic cell death that occurs in the mesenchymal tissue of E8.5 mutant embryos (Fig. 2P,Q), thereby disrupting further tissue differentiation.

***Ldb1* null mutant phenotype: defects in extraembryonic tissues**

Defects in the development of extraembryonic tissues became apparent in *Ldb1* null mutant embryos as they approached the neural-fold stage (E8.5). The yolk sac failed to expand around the fetus and a large portion of the anterior part of the embryo developed outside the yolk sac (Fig. 2O). The development of blood islands and primordial germ cells (PGCs) were also defective in the mutant yolk sac. Benzidine, specific for hemoglobinized erythroid cells, aided in the identification of vitelline blood vessels. In contrast to wild-type (Fig. 3A), mutant embryos lacked any sign of hematopoietic development (Fig. 3B). Identification of PGCs was based on their high alkaline phosphatase activity; these were well developed in the wild-type embryo at E7.5 (Fig. 3C) (see also magnified cells in the inset). However, cells showing this staining were either absent (Fig. 3D) or greatly reduced in *Ldb1*^{-/-} mutants. Another mesoderm-derived structure, the allantois, was also defective and in a few instances entirely absent. Where present, the allantois had become largely detached from the wall of the exocoelomic cavity and was posteriorly displaced by E7.75 (compare Fig. 3E and F). In addition, it appeared to have lost contact with the amnion (Fig. 3F). By E8.5 the tissue had grown towards the chorion but failed to make contact with it.

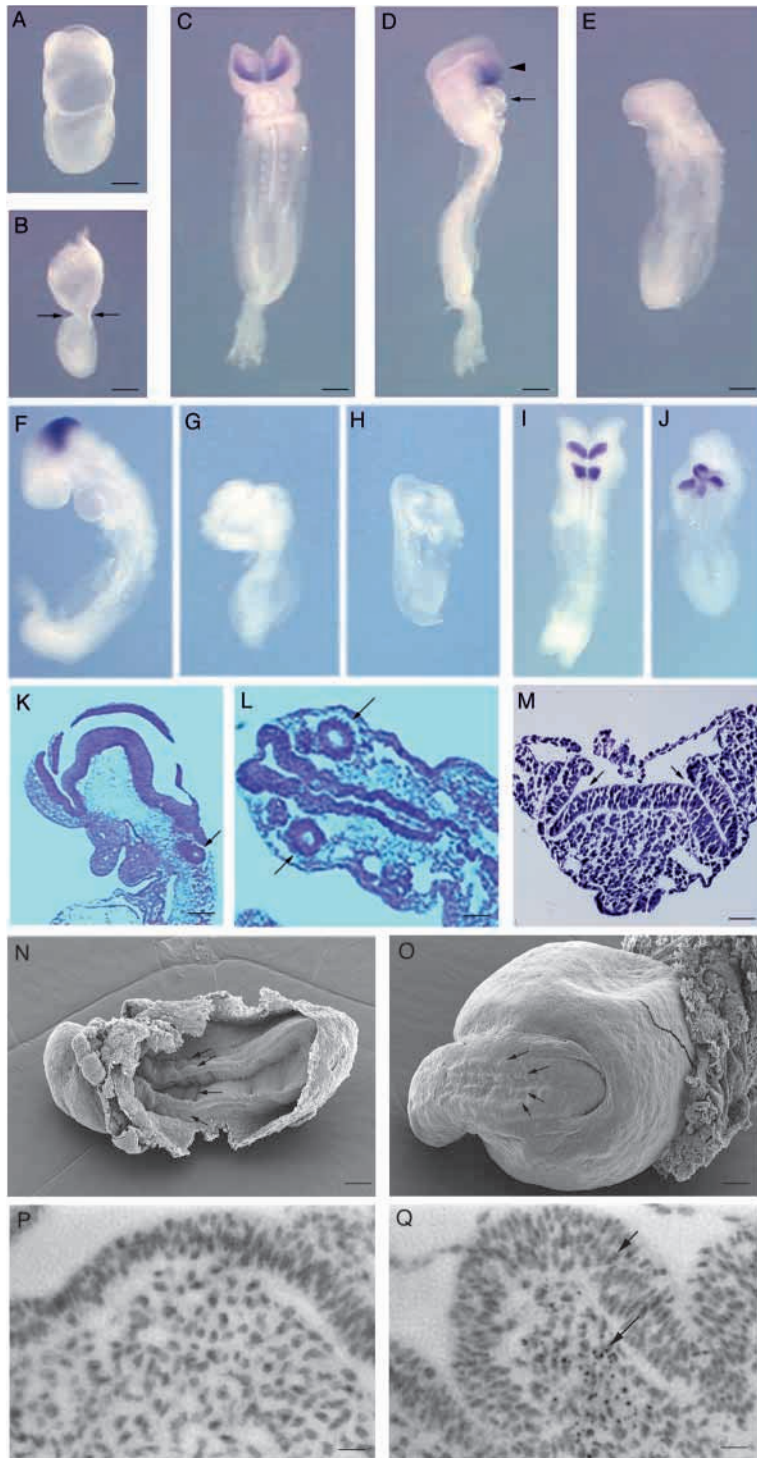


Fig. 2. Anterior-posterior axis phenotypes of *Ldb1* null mutant embryos. (A) Wild-type and (B) mutant E7.5 embryos. A constriction at the embryonic-extraembryonic junction of the mutant embryo is clearly visible (arrows in B). (C-E) E8.5 embryos showing in situ expression patterns of the forebrain marker *Six3*. Frontal (C) and lateral (D) views of a wild-type embryo, showing heart (arrow) and head (arrowhead) structures. Frontal view (ventral side up, E) of an E8.5 mutant embryo with defects in head and heart development, truncation of forebrain structures and absence of *Six3* expression. (F-H) *En2* expression that marks midbrain-hindbrain boundary at E8.5 is present in a wild-type embryo (F) but absent in mutant embryos (G,H). (I,J) *Krox2* expression marking rhombomeres 3 and 5 in wild-type (I) and mutant (J) embryos. Expression of this gene shows partial duplication of rhombomeres 3 and 5 in the mutant (J). (K,L) Hematoxylin and Eosin-stained horizontal sections of E8.5 wild-type and mutant embryos, respectively. The mutant embryo (L) lacks all head structures anterior of the otic vesicles (arrows). The kinks in the neural tube indicate defective longitudinal extension of the neural epithelium. (M) Hematoxylin and Eosin-stained cross section taken from the trunk level of an E8.5 mutant embryo showing abnormal development of two neural grooves (arrows) within a single continuous neuroepithelial layer. (N,O) Scanning electron micrographs presenting ventral (N) and dorsal (O) views of an E8.5 mutant embryo. Abnormal development of four rows of somites is indicated with arrows. (P,Q) TUNEL staining of histological sections taken from comparable regions of E8.5 wild-type and mutant embryos, respectively. Arrows point to extensive cell death in the mesenchyme, and to a lesser degree in the neuroepithelium, of the mutant embryo (Q). The scale bars represents 100 μ m in A-J,N,O; 25 μ m in K,L; 10 μ m in M; and 2 μ m in P,Q.

cardiogenic precursor cells that form the cardiac crescent at the headfold stage (Lints et al., 1993). A marked reduction in *Nkx2.5* expression pattern was observed in *Ldb1*^{-/-} embryos suggesting that the mutant embryos fail to develop a proper cardiac crescent (compare Fig. 4A and B). Heart progenitor cells can be recognized as early as E6.5-7.0 by virtue of expression of the bHLH transcription factor gene *Mesp1* in the early ingressing part of the mesoderm (Saga et al., 1996; Saga et al., 1999). *Mesp1*-expressing nascent mesoderm is fated to become extraembryonic and cranial-cardiac tissue. These cells cease to express *Mesp1* at subsequent stages of gastrulation. However, fate-mapping experiments show migration of the most anterior mesodermal cells expressing *Mesp1* to the heart field (Saga et al., 1999).

The *Mesp1* mRNA is the earliest molecular marker for heart precursor cells known to date. At E7.0, expression of *Mesp1* in *Ldb1* null mutant embryos typically assumes an abnormal 'inverted V' shaped pattern, and the migration of the *Mesp1*-expressing mesodermal cells appears to be restricted to two lateral paths in proximal regions of the embryo (compare Fig. 4C and D). The proximal location of the *Mesp1*-expressing cells may suggest that the mutant embryos lack heart and craniofacial mesoderm that are derived from the distal part of the primitive streak and migrate along an anterior-distal path.

Molecular analyses of the heart phenotype

The heart phenotype of embryos lacking *Ldb1* gene function was characterized with the help of marker analyses performed at critical stages of heart development. Prospective cardiac mesodermal cells invaginate through the primitive streak and migrate and spread out together with cranial mesoderm. Subsequently the bilaterally symmetric cardiac precursors migrate and converge at the midline of the embryo to form the cardiac crescent. *Nkx2.5*, a homeobox gene, is expressed in the

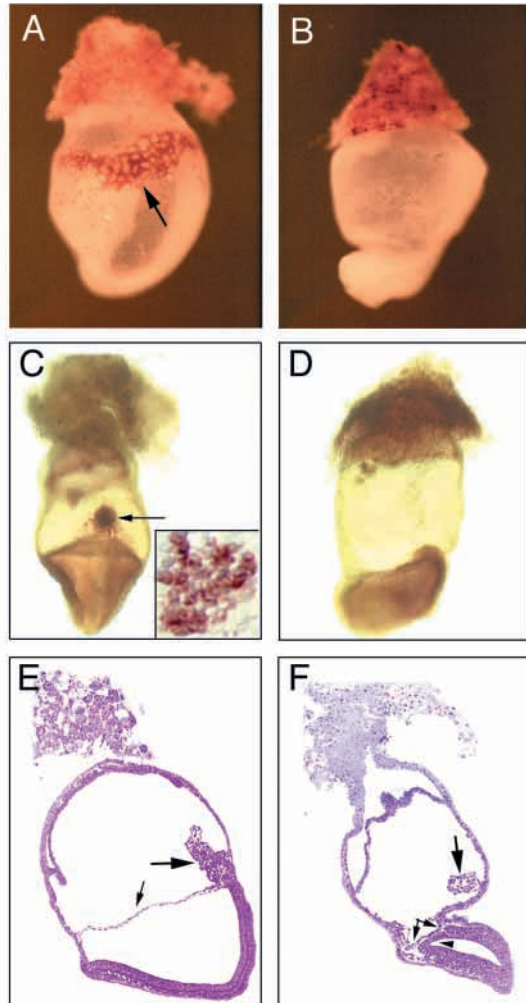


Fig. 3. Defects in extraembryonic tissue development of the *Ldb1* mutant. (A,B) Benzidine staining reveals development of a network of blood islands and primitive vessels (arrow) in the wild-type conceptus at E8.5 (A), which do not exist in the *Ldb1*^{-/-} mutant (B). (C,D) Alkaline phosphatase staining of a wild-type and a mutant E7.5 conceptus, respectively. Primordial germ cells at the base of the allantois are stained in the control (arrow in C, magnified in the inset), while this signal is absent in the mutant (D). (E,F) Extraembryonic tissue morphology. The mesodermal and ectodermal layers (arrow) of the amnion are properly extended at the embryonic/extraembryonic junction of a wild-type embryo (E). During its outgrowth the allantois maintains contact with the embryonic tissue (large arrow in E). In the *Ldb1*^{-/-} mutant embryo (F) the ectodermal layer (arrowhead) of the amnion fails to expand, thus creating a constriction at the embryonic-extraembryonic junction. Although the mesodermal layer of the amnion is expanded, it fails to extend at the constricted embryonic/extraembryonic junction and forms pockets at the anterior and posterior ends (small arrows in F). The mutant allantois (large arrow in F) appears to have lost contact with the embryonic tissue.

This defect in the generation and/or migration of the *Mesp1*-expressing heart progenitor cells may also account for the reduction in *Nkx2.5* expression in the anterior cardiac field at E7.75 (not shown). Our marker analyses thus suggest that the heart phenotype in the *Ldb1* null mutant is an early

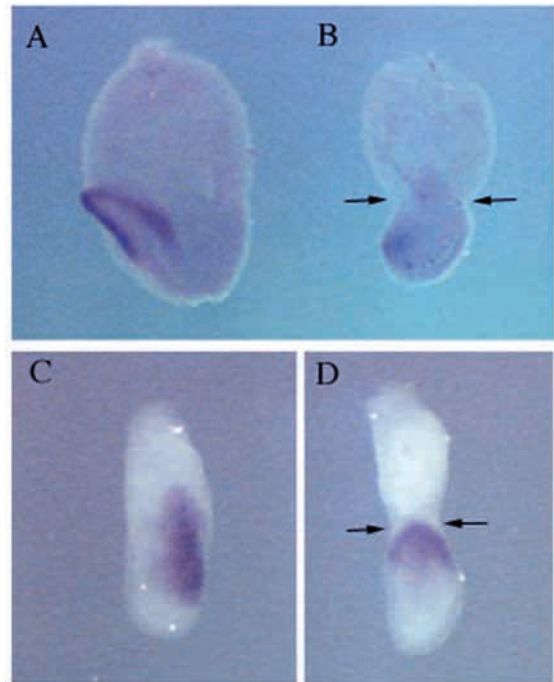


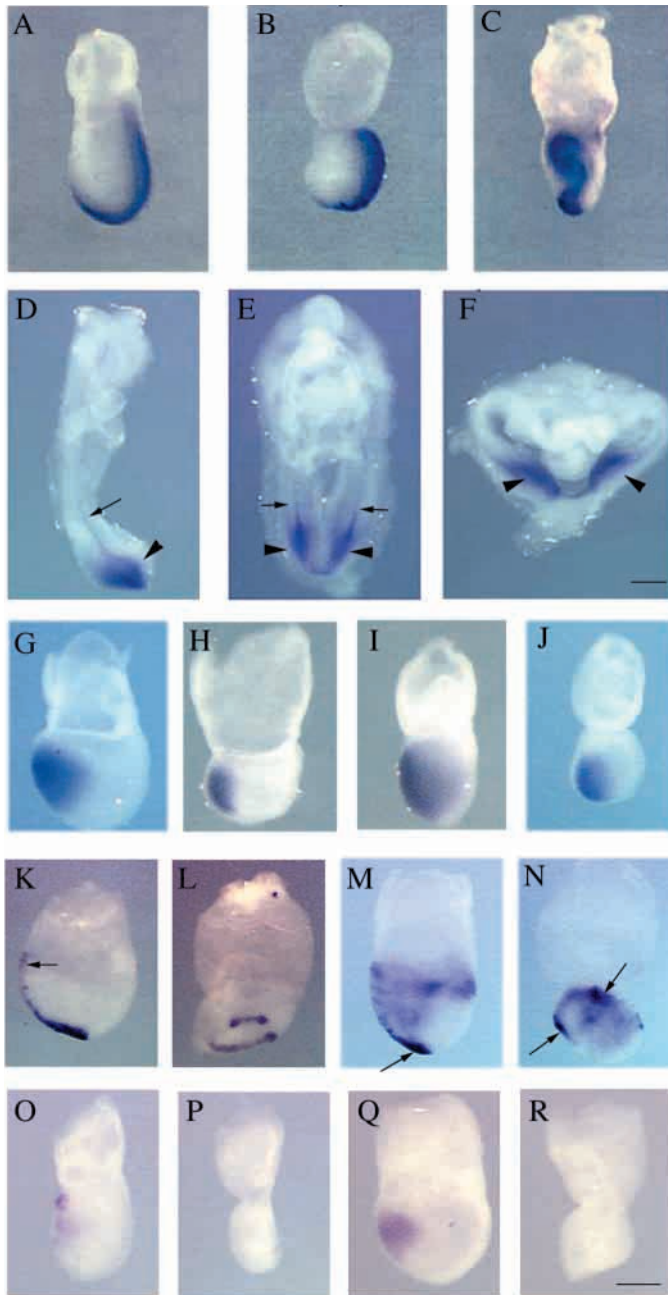
Fig. 4. Expression of heart markers. (A,B) *Nkx2.5* expression at E7.75. At this stage *Nkx2.5* is normally expressed in the heart precursor cells that form a crescent surrounding the heart field (A). The crescent shaped region of *Nkx2.5* expression is absent in a representative mutant embryo shown in B. (C,D) *Mesp1* expression in gastrulating embryos. In the wild-type E6.75 embryo, *Mesp1* expression is seen in early ingressing mesodermal cells along the length of the primitive streak (C). An abnormal V-shaped expression pattern of the *Mesp1* gene in early ingressing mesodermal cells is observed in a stage-matched *Ldb1* null mutant embryo (D; posterior is facing up). The arrows in B and D indicate the embryonic-extraembryonic junction.

developmental defect affecting the generation and/or migration of the earliest recognizable heart precursor cells.

Molecular analyses of the anterior-posterior axis phenotype

We used an extensive array of markers to analyze defects in anterior-posterior axis formation in *Ldb1* null mutant embryos. The posterior axis duplication observed in *Ldb1* null mutant embryos was closely examined using *Brachyury* (*T*) as a molecular marker. In wild-type embryos, *T* expression was seen in the primitive streak throughout gastrulation (Fig. 5A), and in the streak and notochord at post-gastrulation stage E8.5 (Fig. 5D). In gastrulating mutant embryos, defects in streak formation were not always obvious (Fig. 5B). However, the twisted streak seen in some of these mutants suggested to us the presence of two overlapping primitive streaks (Fig. 5C). Indeed, we often observed *T* expression in duplicated primitive streak and notochord formations of E8.5 mutant embryos (Figs 5E,F). In spite of this obvious defect, the anterior extension of the primitive streak appears to be normal. This is not the case in other headless mutant embryos, including *Lim1*, *Otx2* and *Hnf3 β* (Kinder et al., 2001).

Head induction from the presumptive anterior neuroectoderm (ANE) requires *Otx2* gene function in the



anterior visceral endoderm (AVE) prior to gastrulation and in the node-derived anterior mesendoderm (AME). We have detected a reduction in the field of *Otx2* expression in E7.75 *Ldb1* null mutant embryos (Fig. 5G,H). Interestingly, this phenotype is accompanied by a loss or reduction in the expression of *Dkk1*. This, in turn, results in a failure of *Hesx1* to be induced in the prospective ANE (Fig. 5Q,R). Given the established role of *Otx2* in head development and the fact that both *Dkk1* and *Hesx1* act downstream of *Otx2*, our data suggest that a disruption in an *Otx2*-mediated pathway may be the underlying cause for the head phenotype observed in *Ldb1* null mutant embryos.

Hnf3β is a marker for the node and its expression extends anteriorly to the migrating axial mesendoderm that includes the AME cells. *Hnf3β* expression in the mutant was duplicated and

Fig. 5. Marker analyses of anterior-posterior axis formation. (A–C), *Brachyury* (*T*) expression in E7.5 embryos. The embryo shown in B is one of about 60% (32/56) of the *Ldb1* mutant embryos in which proximal-distal extension of the primitive streak appears normal. The embryo shown in C represents mutant embryos in which the expression pattern of *T* is abnormal. In this lateral view we observe a twisted expression domain of *T*, with seemingly normal distal extension. (D–F) *T* expression in E8.5 embryos. (D) Wild-type *T* expression pattern marking the region of the primitive streak (arrowhead) and the notochord (arrow). (E,F), *Ldb1* null mutant embryos with two primitive streaks (arrowheads) connected distally. Two notochords are visible as well (arrows). (G–J), *Otx2* expression at E7.75 (G,H) and E7.5 (I,J) is restricted in the mutant (H,J) compared to the wild type (G,I). (K,L), *Hnf3β* expression in E7.75 embryos. Two posterior expression domains were found in the mutant (L). (K) The wild-type expression of *Hnf3β* in anteriorly migrated endomesodermal cells is indicated by an arrow. This expression domain is absent in the mutant embryo (L). (M,N), *Lim1* expression at E7.5 showing presence of one node in the wild-type (M, arrow) and two nodes in the mutant (N, arrows). (O,P) *Dkk1* expression at mid-streak stage is absent in the mutant embryo (P). (Q,R), *Hesx1* expression at E7.75 is not detectable in the ANE of the mutant. The scale bars represent 100 μm.

failed to extend to the anterior-most aspect of the mutant embryos (Fig. 5K,L). It is likely that the duplicated expression patterns may have developed from duplicated nodes. This is supported by our *Lim1/Lhx1* expression analysis that shows two distinct nodes in the mutant (compare Fig. 5M and N). Note that the probe used in this study confirms the published *Lim1/Lhx1* expression pattern in wild-type embryos (Tsang et al., 2000). However, a small segment of the probe overlaps with the sequence of the closely related *Lim5/Lhx5* gene. Therefore we cannot exclude the possibility that the expression pattern detected with this probe may correspond to *Lhx5*. Nonetheless, our in situ analysis clearly reveals the presence of two nodes in *Ldb1* mutant embryos.

Taken together our results suggest that the anterior truncation of *Ldb1* null mutant embryos is the consequence of a disruption of *Otx2* gene function in the head organizer tissue while the posterior axis duplication phenotype is the outcome of an early node partitioning event.

Molecular mechanism of *Ldb1* gene function

Wnt pathways play an essential role in anterior-posterior axis patterning (McMahon and Moon, 1989; Popperl et al., 1997; Zheng et al., 1997; Liu et al., 1999). Anterior truncation and posterior duplication of the *Ldb1* null mutant axis are reminiscent of phenotypes resulting from overactivation of Wnt pathways (Pöpperl et al., 1997; Borello et al., 1999). We therefore examined the potential role of *Ldb1* in regulating Wnt. *Wnt* overactivation can be achieved either through upregulation of *Wnt* functions or downregulation of Wnt inhibitors. We focused our attention on those *Wnt* genes and inhibitors that are expressed in the early embryo and may play crucial roles in development of structures along the anterior-posterior axis. Our analysis of *Ldb1*^{-/-} embryos failed to detect an increase in steady-state levels of *Wnt3*, *Wnt3a* or *Wnt8* transcripts (data not shown). The *Wnt* inhibitor genes that are expressed during gastrulation include *Dkk1* (Glinka et al., 1998), *Cerberus-like* (*Cer1*) (Belo et al., 1997) and the three secreted Frizzled-related genes *Sfrp1* (Hogan et al., 1998),

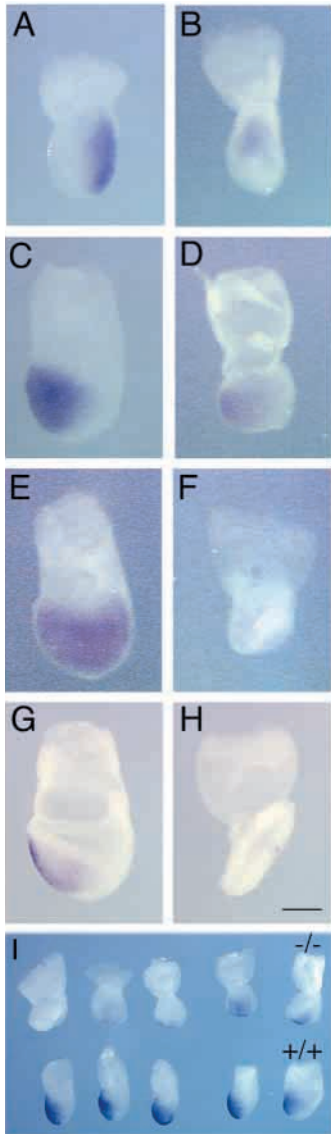


Fig. 6. Expression of *Wnt* inhibitors in E7.5 embryos. Wild-type embryos are on the left, *Ldb1*^{-/-} mutants on the right. (A,B) *Frzb* expression. Expression is undetectable in the primitive streak and the prospective cardiac mesoderm regions of the mutant. (C,D), Expression of *Sfrp1*. The signal is greatly reduced in the anterior ectoderm of the mutant. (E,F) Expression of *Sfrp2*. This signal is absent in the mutant. (G,H) *Cer1* expression. The signal, marking the AVE, the axial mesendoderm and the definitive endoderm of late streak embryos, is absent in the mutant. (I) Variation in the expression level of the *Cer1* gene in *Ldb1* mutant and wild-type embryos. The scale bar represents 100 μ m.

Sfrp2 (Leimeister et al., 1998), and *Frzb/Sfrp3* (Hoang et al., 1998). At E7.5, *Frzb/Sfrp3* expression is seen in the primitive streak and prospective cardiac mesoderm of wild-type embryos (Fig. 6A) (Hoang et al., 1998). At this stage *Sfrp1* expression is found in the ectodermal tissue located anterior to the migrating head process (Fig. 6C) (Hoang et al., 1998). By contrast, the expression domain of *Sfrp2* is much broader, encompassing medial and distal embryonic tissues (Fig. 6E) (Leimeister et al., 1998). At late streak stages, *Cer1* expression is seen in the AVE, axial mesoderm and in definitive endodermal cells of wild-type embryos (Fig. 6G) (Belo et al., 1997). Our analysis showed that expression of all five *Wnt* inhibitor genes tested is compromised in the mutants (Fig. 6B,D,F,H,I). While steady-state transcript levels of all *Wnt* inhibitors tested were reduced when compared to those of controls, the degree of reduction varied between individual mutants, as exemplified in Fig. 6I. Since *Wnt* proteins are known to act as posteriorizing agents (reviewed by Niehrs, 1999), the apparent downregulation of *Wnt* inhibitors suggests the possibility that the headless phenotype of the *Ldb1* null

mutants may result from overactivation of *Wnt* pathways along the anterior-posterior axis.

Detection of maternally deposited *Ldb1* mRNA in the wild-type oocyte

The *Drosophila* *Ldb1* homolog *Chip* is not only expressed zygotically but is also provided maternally (Morcillo et al., 1997). Maternal *Chip* mRNA is required for embryonic development before the onset of zygotic expression. Embryos lacking maternal mRNA are unable to form segments and die early in embryonic development while embryos lacking zygotic *Chip* are able to form segments. These embryos hatch but die as larvae (Morcillo et al., 1996). We have considered the analogous possibility that maternal *Ldb1* mRNA may play a role in early mouse development. Our RT-PCR analyses of RNA samples extracted from eggs or zygotes before the onset of zygotic expression clearly showed deposition of maternal *Ldb1* mRNA in early mouse embryos (Fig. 7). Although we were unable to detect the presence of maternal *Ldb1* mRNA in E7.5 mutant embryos, the possibility remains that protein translated from maternally deposited mRNA may support early stages of development in the zygotic null mutants. Alternatively, or in addition, partial functional redundancy may exist between *Ldb1* and *Ldb2*, the second member of the *Ldb* family (Agulnick et al., 1996; Jurata et al., 1996; Bach et al., 1997). It is possible that variables such as these may underlie the incomplete penetrance of phenotypes such as posterior axis duplication.

DISCUSSION

Ldb1 gene function is required for anterior patterning of the gastrulating embryo

The phenotype of the *Ldb1* null mutant mouse embryo has uncovered major functions of the *Ldb1* gene in the establishment of the primary anterior-posterior body axis. All mutant embryos show a disruption of anterior development as manifested by a truncation of anterior head structures and a lack of heart and foregut anlagen. The AVE, an extraembryonic tissue, has been strongly implicated in conferring initial rostral identity to the embryo before gastrulation (Thomas and Beddington, 1996). As gastrulation proceeds, head induction depends on crosstalk between cells of the AVE, the AME and the ANE that converge near the rostral end of the anterior-posterior axis (Shawlot et al., 1999; Tam and Steiner, 1999). The homeobox-containing transcriptional regulators *Lim1/Lhx1* and *Otx2* play indispensable roles in head development as judged from the respective null mutant 'headless' phenotypes (Shawlot and Behringer, 1995; Acampora et al., 1995; Matsuo et al., 1995; Ang et al., 1996). *Ldb1* has been implicated to act as a cofactor for both of these transcription factors (Agulnick et al., 1996; Bach et al., 1997). Consistent with this we have demonstrated that in the head organizer tissue of *Ldb1* null mutant embryos the *Otx2* downstream pathway is affected. We have detected loss or reduction in mRNA expression levels of the *Otx2* downstream genes *Dkk1* and *Hesx1*. Since *Otx2* function is known to be required for induction of its own expression in the prospective anterior neuroectodermal tissue (Ang et al., 1994; Acampora

et al., 1998), the observed reduction of the *Otx2* expression domain in *Ldb1* mutant embryos may further suggest a defect in *Otx2* downstream pathways. *Otx* gene products can interact both with *Ldb1* and with *Lim1/Lhx1* (Bach et al., 1997; Nakano et al., 2000). Therefore, the head phenotype in *Ldb1* mutant embryos may, at least in part, be attributable to a disruption of pathways controlled by *Otx2* and/or *Lim1/Lhx1*.

Ablation of *Ldb1* causes posterior axis duplication

The axis duplication that we observed in a majority of *Ldb1* null mutant embryos is reminiscent of a similar phenotype observed in embryos that carry homozygous mutations at the *fused* locus (Gluecksohn-Schoenheimer, 1949; Perry et al., 1995). Axis duplication was also observed in *Lim1/Lhx1* null mutant embryos. Here, as in our case, the duplication affected only the posterior region, resulting in a Y-shaped structure fused at the truncated anterior end (Shawlot and Behringer, 1995). Posterior axis duplication can be induced by grafting node tissue to a posterior-lateral position in the gastrulating mouse embryo (Beddington, 1994). Using the node marker *Hnf3 β* and *Lim1/Lhx1* (Ang and Rossant, 1994), we were able to determine that abnormal generation of a duplicated node structures is the underlying cause for posterior axis duplication in the *Ldb1* mutant. The fact that functional ablation of either *Ldb1* or *Lim1/Lhx1* causes anterior truncation and can also induce partial posterior axis duplication may be taken as a genetic indication that an interaction of these two factors is essential for proper anterior-posterior axis development, from head to tail.

Furthermore, we noted that expression of several Wnt inhibitors is downregulated in *Ldb1* mutant embryos. It is important to note that the function of Cer1 (Belo et al., 2000), and possibly that of other Wnt inhibitors as well, is dispensable during mouse embryonic development, suggesting that functional redundancy may exist. The severe phenotypic abnormalities observed in *Ldb1* null mutant embryos may reflect the simultaneous functional obstruction of several Wnt inhibitors.

A number of recent studies have revealed a role of Wnt pathways in anterior-posterior axis formation (reviewed by Yamaguchi, 2001). Frequent posterior axis duplication is seen in transgenic mice over-expressing chicken *Wnt8c* (Pöpperl et al., 1997). *Wnt3* has been implicated in anterior-posterior axis formation because null mutant embryos lack the primitive streak and do not form mesoderm and definitive endoderm (Liu et al., 1999). Loss-of-function analysis of *Dkk1* demonstrated that this Wnt inhibitor is required for rostral development (Mukhopadhyay et al., 2001). Over-expression of the Wnt inhibitor *Frzb* during early mouse development leads to reduction in the size of caudal structures (Borello, 1999). Furthermore, *Frzb* interferes with the ability of *Xwnt8* to induce double axes in *Xenopus* (Leyns et al., 1997; Wang et al., 1997). Whether proper regulation of Wnt inhibitors by *Ldb1* (in conjunction with interacting LIM-homeodomain factors) is a prerequisite for regulation of Wnt pathways during anterior-posterior axis development remains to be determined.

Ldb1 plays a critical role in heart formation

In *Ldb1* null mutant embryos heart development is compromised at early stages of development. Our data suggest that the *Ldb1* gene function is essential for proper allocation

of the *Mesp1*-expressing cardiac mesoderm to the heart field. In the chick, heart mesoderm is induced by the signals from the anterior endoderm. The heart precursor cells are in contact with presumptive anterior endoderm throughout their migration from the streak into the lateral plate (Garcia-Martinez and Schoenwolf, 1993). Abnormal migration of the heart mesoderm to a lateral-proximal region of the mutant embryo may therefore abolish inductive interaction of this tissue with anterior endoderm.

BMP signaling is known to be essential, but not sufficient, for heart formation (Schultheiss et al., 1997; Andree et al., 1998). Presently additional factors are being examined in the chick embryo. One of these is Crescent, a Frizzled-related protein that inhibits Wnt8c and is expressed in the anterior endoderm during gastrulation. Ectopic expression of *Crescent* in the posterior lateral plate mesoderm leads to development of ectopic heart tissue with beating cardiomyocytes. The Wnt inhibitor *Dkk1* similarly induces heart-specific gene expression from anterior mesoderm when ectopically expressed. Furthermore, ectopic Wnt signals can repress heart formation from anterior mesoderm in vitro and in vivo. These results led to the conclusion that inhibition of Wnt signaling is required for heart development in the chick (Marvin et al., 2001). Similarly, Wnt antagonism initiates cardiogenesis in *Xenopus* (Schneider and Mercola, 2001). While this may also hold true for the mouse, there are presently no data that would support this notion. A vertebrate homolog of *Crescent* has not yet been identified. Furthermore, disruption of mouse *Dkk1* gene function does not lead to a disruption of heart development (Mukhopadhyay et al., 2001). It is, of course, entirely possible that mammalian heart development requires the activity of more than one Wnt inhibitor and that the loss of *Dkk1* gene function may be compensated by the activity of other Wnt inhibitors that remain to be identified. Finally, it is interesting to note that members of the GATA family of zinc finger transcription factors are required for mouse heart formation (Molkentin et al., 1997). GATA proteins have been detected in nuclear complexes that also contain *Ldb1* (Wadman et al., 1997), in keeping with the possibility that a physical interaction of *Ldb1* with GATA peptides may take place during heart development.

Lack of *Ldb1* gene function leads to defects in the development of extraembryonic structures derived from mesoderm

Malformations of the yolk sac, amnion, primordial germ cells (PGCs) and allantois of the *Ldb1* null mutant conceptus point to severe defects in posterior mesoderm formation. In general these phenotypes may reflect a defect in mesodermal cell migration even though primitive streak extension appears normal in the mutant.

The yolk sac plays a pivotal role in the delivery of nutrients to the embryo prior to fusion of the allantois to the chorion at E9.5 (Cross, 1994), and disruption of yolk sac function causes embryonic lethality (Bielinska, 1999). In our mutants, the yolk sack failed to surround the entire embryo. This is reminiscent of malformations seen in the naturally occurring *kinky* mutant (Gluecksohn-Schoenheimer, 1949), and in *Hnf3 β* (*Foxa2*) (Ang et al., 1996) and *Gata4* (Molkentin, 1997) null mutants. However, the yolk sac phenotype of the *Ldb1* null mutant is distinct from these because the posterior part of the embryo



Fig. 7. Analysis of maternal *Ldb1* expression. Lanes 1-3, RT-PCR analysis for *Ldb1* mRNA. Lane 1, oocytes; lanes 2 and 3, E7.5 embryos. *Ldb1* mRNA is detected in wild-type (lane 2), but not in *Ldb1* null mutant embryos (lane 3). Lanes 4-6, expression of control mRNA. The control mRNA is absent in the egg (lane 4), but present in E7.5 wild-type (lane 5) and *Ldb1* mutant (lane 6) embryos.

develops within the yolk sac whereas the anterior region does not.

Within the *Ldb1* null mutant yolk sac, the development of blood islands is compromised. In the wild-type controls, blood islands appear at E7.5 in the extraembryonic mesoderm of the yolk sac. They represent areas of primitive hematopoiesis and vasculogenesis that develop into a vascular network by E8.5. Defects of early hematopoiesis and the development of blood islands have also been observed in *Bmp4* null mutants that, like our *Ldb1* null mutants, are characterized by defective mesodermal differentiation (Winnier, 1995). *Ldb1* can form a transcriptional complex with *Lmo2*, *Tal1*, *Gata1* and *E47*. Functional ablation of the first three of these four proteins by targeted gene disruption results in severe defects in hematopoiesis (Wadman et al., 1997). The absence of blood islands in the *Ldb1*^{-/-} mutant may thus be explained by assigning *Ldb1* an essential role as a co-factor in early transcriptional events that initiate yolk sac hematopoiesis.

Also compromised in the *Ldb1* null mutant yolk sac is the formation of the primordial germ cells (PGCs). These cells are characterized by a high alkaline phosphatase activity and can be visualized starting around E7.25 in the mesodermal part of the yolk sac at the base of the allantois, posterior to the primitive streak (Chiquoine, 1954; Lawson and Hage, 1994). Shortly thereafter, they follow a migration path along the hindgut endoderm and hindgut mesentery to the urogenital ridge where the gonad forms. Cell transplantation studies have suggested that PGC development requires a distinct micro-environment in the proximal epiblast (Tam and Zhou, 1996). *Bmp4* (Lawson, 1999), *Bmp8b* (Ying, 2000), *Hnf3β* and *Lim1/Lhx1* (Tsang, 2001) appear to be essential functional components of this environment, as their loss results in defects of PGC formation. Since *Ldb1* is a known co-factor of *Lim1/Lhx1* activity and PGC development is similarly compromised in *Ldb1* and in *Lim1/Lhx1* null mutants (Tsang, 2001), impairment of *Lim1/Lhx1* activity is a likely cause of the PGC phenotype. In addition, *Ldb1* activity may be required for the proper temporal and spatial expression of some or all of the other aforementioned factors known to play a role in PGC development. This is suggested by the fact that *Bmp4* and *Hnf3β* were mis-expressed in the *Ldb1* null mutant (data not shown).

A further defect in the development of extraembryonic tissues was seen in the allantois of the *Ldb1* null mutant conceptus. The wild-type allantois is derived from posterior streak mesoderm and extends into the exo-coelomic cavity. Loss-of-function studies have implicated a number of genes in this process, including *Brachyury* (*T*) (Chesley, 1935), *Hnf3β* (Ang et al., 1994), *VCAM-1* (Gurtner et al., 1995), *Otx2* (Ang et al., 1996), *Bmp4* (Lawson, 1999) and *Lim1/Lhx1* (Tsang,

2001). The *Ldb1* null mutants form an extra-coelomic cavity, indicating that posterior mesoderm has reached the correct extraembryonic location and has lined the exocoelom. However, after this initial step, growth of the allantois is arrested and fusion with the chorion does not occur.

We observed a marked constriction between the embryonic and extraembryonic portions of the E6.5-E7.5 *Ldb1* null mutant. Similar constrictions have been observed in mutants that are homozygous for deletions in *Hnf3β* (Ang and Rossant, 1994; Weinstein et al., 1999), *Lhx1/lim1* (Shawlot and Behringer, 1995; Shawlot et al., 1999), *Otx2* (Ang et al., 1996) and *Nodal* (Varlet et al., 1997). During subsequent development, deficiencies in rostral structures are noted in all of these mutants. The constriction has been viewed as an indication of defective cell movement during gastrulation (Foley and Stern, 2001). Alternatively, it may reflect a failure of visceral endoderm to proliferate or to confer proper morphogenetic signals to the underlying embryonic ectoderm (Dufort et al., 1998). In the *Ldb1* null mutant, the amnion fails to extend normally. As the volume of the epiblast and that of the exocoelomic cavity increase rapidly after E6.5, a foreshortening of the amnion between these two regions of the conceptus may prevent lateral outgrowth in the mid-region, resulting in the observed constriction. Nonetheless, the embryonic and extraembryonic portions of the *Ldb1*^{-/-} mutants are separated by the amnion, indicating that the initial formation of the posterior amniotic fold and the subsequent closure of the pro-amniotic canal occur properly. Around E7.25, coinciding with the malformation of the allantois and the PGCs, the expansion of the amnion becomes defective. The amnion consists of two layers, the amniotic mesoderm and the amniotic ectoderm. Our findings suggest that the failure of the amnion to extend appropriately is due to a defect in the ectodermal layer of the amnion (Fig. 3F), because the amniotic mesoderm forms pockets near the anterior and posterior end of the amniotic layer, while the ectoderm fails to expand properly. This indicates that there is an excess of tissue in the mesodermal layer relative to the ectodermal layer, making it unlikely that the mesodermal layer is primarily responsible for the constriction. However, as the allantois and PGCs are defective in the *Ldb1* mutant, the development of the amniotic mesoderm, which is also derived from the posterior primitive streak, may nonetheless be defective as well.

Conclusion

Loss of zygotic *Ldb1* function results in a multi-faceted phenotype that reveals a requirement of *Ldb1* during early post-implantation development of the mouse embryo, including formation of the anterior-posterior axis, the anlage of the heart and the elaboration of major mesoderm-derived extra-embryonic structures. The mutant phenotype very likely reflects the malfunction of a diverse array of transcription factors whose action depends on a functional *Ldb1* co-factor. This, in turn, may affect major signaling events, including those mediated by the canonical Wnt pathway.

We thank Drs S. L. Ang, M. Kuehn, M. M. Shen and P. P. Tam for helpful suggestions; and Drs S. L. Ang, C. Chin, E. M. DeRobertis, M. Kuehn, G. Oliver, F. P. Luyten, Y. Saga and Y. Ying for materials. This work was partially supported by a Feodor Lynen Research

Fellowship from the Alexander von Humboldt Foundation, Germany, to A. T. and by NIH Grant HD36847 to K. M. Downs.

REFERENCES

- Acampora, D., Mazan, S., Lallemand, Y., Avantaggiato, V., Maury, M., Simeone, A. and Brulet, P.** (1995). Forebrain and midbrain regions are deleted in *Otx2*^{-/-} mutants due to a defective anterior neuroectoderm specification during gastrulation. *Development* **121**, 3279-3290.
- Acampora, D., Avantaggiato, V., Tuorto, F., Briata, P., Corte, G. and Simeone, A.** (1998). Visceral endoderm-restricted translation of *Otx1* mediates recovery of *Otx2* requirements for specification of anterior neural plate and normal gastrulation. *Development* **125**, 5091-5104.
- Agulnick, A. D., Taira, M., Breen, J. J., Tanaka, T., Dawid, I. B. and Westphal, H.** (1996). Interactions of the LIM-domain-binding factor *Ldb1* with LIM homeodomain proteins. *Nature* **384**, 270-272.
- Andree, B., Duprez, D., Vorbusch, B., Arnold, H. H. and Brand, T.** (1998). BMP-2 induces ectopic expression of cardiac lineage markers and interferes with somite formation in chicken embryos. *Mech. Dev.* **70**, 119-131.
- Ang, S. L., Conlon, R. A., Jin, O. and Rossant, J.** (1994). Positive and negative signals from mesoderm regulate the expression of mouse *Otx2* in ectoderm explants. *Development* **120**, 2979-2989.
- Ang, S. L. and Rossant, J.** (1994). HNF-3 beta is essential for node and notochord formation in mouse development. *Cell* **78**, 561-574.
- Ang, S. L., Jin, O., Rhinn, M., Daigle, N., Stevenson, L. and Rossant, J.** (1996). A targeted mouse *Otx2* mutation leads to severe defects in gastrulation and formation of axial mesoderm and to deletion of rostral brain. *Development* **122**, 243-252.
- Bach, I., Carriere, C., Ostendorff, H. P., Andersen, B. and Rosenfeld, M. G.** (1997). A family of LIM domain-associated cofactors confer transcriptional synergism between LIM and *Otx* homeodomain proteins. *Genes Dev.* **11**, 1370-1380.
- Bach, L.** (2000). The LIM domain: regulation by association. *Mech. Dev.* **91**, 5-17.
- Beddington, R. S. P.** (1994). Induction of a second neural axis by the mouse node. *Development* **120**, 613-620.
- Beddington, R. S. P. and Robertson, E. J.** (1998). Anterior patterning in mouse. *Trends Genet.* **14**, 277-284.
- Belo, J. A., Bouwmeester, T., Leyns, L., Kertesz, N., Gallo, M., Follettie, M. and De Robertis, E. M.** (1997). Cerberus-like is a secreted factor with neutralizing activity expressed in the anterior primitive endoderm of the mouse gastrula. *Mech. Dev.* **68**, 45-57.
- Belo, J. A., Bachiller, D., Agius, E., Kemp, C., Borges, A. C., Marques, S., Piccolo, S. and DeRobertis, E. M.** (2000). Cerberus-like is a secreted BMP and nodal antagonist not essential for mouse development. *Genesis* **26**, 265-270.
- Bielineska, M., Narita, N. and Wilson, D. B.** (1999). Distinct roles for visceral endoderm during embryonic mouse development. *Int. J. Dev. Biol.* **43**, 183-205.
- Borello, U., Coletta, M., Tajbakhsh, S., Leyns, L., De Robertis, E. M., Buckingham, M. and Cossu, G.** (1999). Transplacental delivery of the Wnt antagonist *Frzb1* inhibits development of caudal paraxial mesoderm and skeletal myogenesis in mouse embryos. *Development* **126**, 4247-4255.
- Bouillet, P., Oulad-Abdelghani, M., Ward, S. J., Bronner, S., Chambon, P. and Dolle, P.** (1996). A new mouse member of the Wnt gene family, *mWnt-8*, is expressed during early embryogenesis and is ectopically induced by retinoic acid. *Mech. Dev.* **58**, 141-152.
- Breen, J. J., Agulnick, A. D., Westphal, H. and Dawid, I. B.** (1998). Interactions between LIM domains and the LIM domain-binding protein *Ldb1*. *J. Biol. Chem.* **273**, 4712-4717.
- Cassata, G., Rohrig, S., Kuhn, F., Hauri, H. P., Baumeister, R. and Burglin, T. R.** (2000). The *Caenorhabditis elegans* *Ldb/NLI/Clim* orthologue *Ldb-1* is required for neuronal function. *Dev. Biol.* **226**, 45-56.
- Chesley, P.** (1935). Development of the short-tailed mutant in the house mouse. *J. Exp. Zool.* **70**, 429-453.
- Chiquoine, A. D.** (1954). The identification, origin, and migration of the primordial germ cells in the mouse embryo. *Anat. Rec.* **118**, 135-146.
- Cross, J. C., Werb, Z. and Fisher, S. J.** (1994). Implantation and the placenta: key pieces of the development puzzle. *Science* **266**, 1508-1518.
- Dawid, I. B., Breen, J. J. and Toyama, R.** (1998). LIM domains: multiple roles as adapters and functional modifiers in protein interactions. *Trends Genet.* **14**, 156-162.
- de Souza, F. S. J. and Niehrs, C.** (2000). Anterior endoderm and head induction in early vertebrate embryos. *Cell Tissue Res.* **300**, 207-217.
- Dufort, D., Schwartz, L., Harpal, K. and Rossant, J.** (1998). The transcription factor HNF3beta is required in visceral endoderm for normal primitive streak morphogenesis. *Development* **125**, 3015-3025.
- Foley, A. C. and Stern, C. D.** (2001). Evolution of vertebrate forebrain development: how many different mechanisms? *J. Anat.* **199**, 35-52.
- Garcia-Martinez, V. and Schoenwolf, G. C.** (1993). Primitive-streak origin of the cardiovascular system in avian embryos. *Dev. Biol.* **159**, 706-719.
- German, M. S., Wang, J., Chadwick, R. B. and Rutter, W. J.** (1992). Synergistic activation of the insulin gene by a LIM-homeo domain protein and a basic helix-loop-helix protein: building a functional insulin minihancer complex. *Genes Dev.* **6**, 2165-2176.
- Glinka, A., Wu, W., Delius, H., Monaghan, P. A., Blumenstock, C. and Niehrs, C.** (1998). *Dickkopf1* is a member of a new family of secreted proteins and functions in head induction. *Nature* **391**, 357-362.
- Gluecksohn-Schoenheimer, S.** (1949). The effect of a lethal mutation responsible for duplications and twinning in mouse embryos. *J. Exp. Zool.* **110**, 47-76.
- Gurtner, G. C., Davis, V., Li, H., McCoy, M. J., Sharpe, A. and Cybulsky, M. I.** (1995). Targeted disruption of the murine VCAM1 gene: essential role of VCAM-1 in chorioallantoic fusion and placentation. *Genes Dev.* **9**, 1-14.
- Herrmann, B. G.** (1992). Action of the Brachyury gene in mouse embryogenesis. *Ciba Found. Symp.* **165**, 78-86.
- Hoang, B. H., Thomas, J. T., Abdul-Karim, F. W., Correia, K. M., Conlon, R. A., Luyten, F. P. and Ballock, R. T.** (1998). Expression pattern of two Frizzled-related genes, *Frzb-1* and *Sfrp-1*, during mouse embryogenesis suggests a role for modulating action of Wnt family members. *Dev. Dyn.* **212**, 364-372.
- Hobert, O. and Westphal, H.** (2000). Functions of LIM-homeobox genes. *Trends Genet.* **16**, 75-83.
- Jurata, L. W., Kenny, D. A. and Gill, G. N.** (1996). Nuclear LIM interactor, a rhombotin and LIM homeodomain interacting protein, is expressed early in neuronal development. *Proc. Natl. Acad. Sci. USA* **93**, 11693.
- Jurata, L. W. and Gill, G. N.** (1997). Functional analysis of the nuclear LIM domain interactor NLI. *Mol. Cell. Biol.* **17**, 5688-5698.
- Jurata, L. W. and Gill, N.** (1998). Structure and function of LIM domains. *Curr. Top. Microbiol. Immunol.* **228**, 75-113.
- Kinder, S. J., Tsang, T. E., Ang, S. L., Behringer, R. R. and Tam, P. P.** (2001). Defects of the body plan of mutant embryos lacking *Lim1*, *Otx2* or *Hnf3beta* activity. *Int. J. Dev. Biol.* **45**, 347-355.
- Lawson, K. A., Dunn, N. R., Roelen, B. A., Zeinstra, L. M., Davis, A. M., Wright, C. V., Korving, J. P. and Hogan, B. L.** (1999). *Bmp4* is required for the generation of primordial germ cells in the mouse embryo. *Genes Dev.* **13**, 424-436.
- Lawson, K. A. and Hage, W. J.** (1994). Clonal analysis of the origin of primordial germ cells in the mouse. *Ciba Found. Symp.* **182**, 68-84.
- Lints, T. J., Parsons, L. M., Hartley, L., Lyons, I. and Harvey, R. P.** (1993). *Nkx-2.5*: a novel murine homeobox gene expressed in early heart progenitor cells and their myogenic descendants. *Development* **119**, 419-431.
- Liu, P., Wakamiya, M., Shea, M. J., Albrecht, U., Behringer, R. R. and Bradley, A.** (1999). Requirement for *Wnt3* in vertebrate axis formation. *Nature Genet.* **22**, 361-365.
- Leimeister, C., Bach, A. and Gessler, M.** (1998). Developmental expression patterns of mouse *sFRP* genes encoding members of the secreted frizzled related protein family. *Mech. Dev.* **75**, 29-42.
- Leyns, L., Bouwmeester, T., Kim, S. H., Piccolo, S. and De Robertis, E. M.** (1997). *Frzb-1* is a secreted antagonist of Wnt signaling expressed in the Spemann organizer. *Cell* **88**, 747-756.
- Marvin, M. J., Di Rocco, G., Gardiner, A., Bush, S. M. and Lassar, A. B.** (2001). Inhibition of Wnt activity induces heart formation from posterior mesoderm. *Genes Dev.* **15**, 316-327.
- Matsuo, I., Kuratani, S., Kimura, C., Takeda, N. and Aizawa, S.** (1995). Mouse *Otx2* functions in the formation and patterning of rostral head. *Genes Dev.* **9**, 2646-2658.
- McMahon, A. P. and Moon, R. T.** (1989). Ectopic expression of the proto-oncogene *int-1* in *Xenopus* embryos leads to duplication of the embryonic axis. *Cell* **58**, 1075-1084.
- Meyer, A. and Schartl, M.** (1999). Gene and genome duplications in vertebrates: the one-to-four (-to-eight in fish) rule and the evolution of novel gene functions. *Curr. Opin. Cell. Biol.* **11**, 699-704.
- Molkentin, J. D., Lin, Q., Duncan, S. A. and Olson, E. N.** (1997). Requirement of the transcription factor *GATA4* for heart tube formation and ventral morphogenesis. *Genes Dev.* **11**, 1061-1072.

- Morcillo, P., Rosen, C. and Dorsett, D. (1996). Genes regulating the remote wing margin enhancer in the *Drosophila* cut locus. *Genetics* **144**, 1143-1154.
- Morcillo, P., Rosen, C., Baylies, M. K. and Dorsett, D. (1997). Chip, a widely expressed chromosomal protein required for segmentation and activity of a remote wing margin enhancer in *Drosophila*. *Genes Dev.* **11**, 2729-2740.
- Mukhopadhyay, M., Shtrom, S., Rodriguez-Esteban, C., Chen, L., Tsukui, T., Gomer, L., Dorward, D. W., Glinka, A., Grinberg, A., Huang, S. P., Niehrs, C., Belmonte, J. C. and Westphal, H. (2001). Dickkopf1 is required for embryonic head induction and limb morphogenesis in the mouse. *Dev. Cell* **1**, 423-434.
- Nakano, T., Murata, T., Matsuo, I. and Aizawa, S. (2000). OTX2 directly interacts with LIM1 and HNF-3beta. *Biochem. Biophys. Res. Commun.* **267**, 64-70.
- Niehrs, C. (1999). Head in the Wnt. *Trends in Genet.* **15**, 314-319.
- Oliver, G., Mailhos, A., Wehr, R., Copeland, N. G., Jenkins, N. A. and Gruss, P. (1995). Six3, a murine homologue of the sine oculis gene, demarcates the most anterior border of the developing neural plate and is expressed during eye development. *Development* **121**, 4045-4055.
- Perry, W. L. 3rd, Vasicsek, T. J., Lee, J. J., Rossi, J. M., Zeng, L., Zhang, T., Tilghman, S. M. and Costantini, F. (1995). Phenotypic and molecular analysis of a transgenic insertional allele of the mouse Fused locus. *Genetics* **141**, 321-332.
- Pöpperl, H., Schmidt, C., Wilson, V., Hume, C. R., Dodd, J., Krumlauf, R. and Beddington, R. S. (1997). Misexpression of Cwnt8C in the mouse induces an ectopic embryonic axis and causes a truncation of the anterior neuroectoderm. *Development* **124**, 2997-3005.
- Rhinn, M., Dierich, A., Shawlot, W., Behringer, R. R., Le Meur, M. and Ang, S. L. (1998). Sequential roles for Otx2 in visceral endoderm and neuroectoderm for forebrain and midbrain induction and specification. *Development* **125**, 845-856.
- Robards, A. W. and Wilson, A. J., eds (1993). Basic biological preparation techniques for SEM. In *Procedures in Electron Microscopy*, pp. 11.4.1-11.4.17. Chichester: John Wiley & Sons.
- Saga, Y., Hata, N., Kobayashi, S., Magnuson, T., Seldin, M. F. and Taketo, M. M. (1996). MesP1: a novel basic helix-loop-helix protein expressed in the nascent mesodermal cells during mouse gastrulation. *Development* **122**, 2769-2778.
- Saga, Y., Miyagawa-Tomita, S., Takagi, A., Kitajima, S., Miyazaki, J. and Inoue, T. (1999). MesP1 is expressed in the heart precursor cells and required for the formation of a single heart tube. *Development* **126**, 3437-3447.
- Sanchez-Garcia, I. and Rabbitts, T. H. (1994). The LIM domain: a new structural motif found in zinc-finger-like proteins. *Trends Genet.* **10**, 315-320.
- Schneider, V. A. and Mercola, M. (2001). Wnt antagonism initiates cardiogenesis in *Xenopus laevis*. *Genes Dev.* **15**, 304-315.
- Schultheiss, T. M., Burch, J. B. and Lassar, A. B. (1997). A role for bone morphogenetic proteins in the induction of cardiac myogenesis. *Genes and Dev.* **11**, 451-462.
- Shawlot, W. and Behringer, R. R. (1995). Requirement for Lim1 in head-organizer function. *Nature* **374**, 425-430.
- Shawlot, W., Wakamiya, M., Kwan, K. M., Kania, A., Jessell, T. M. and Behringer, R. R. (1999). Lim1 is required in both primitive streak-derived tissues and visceral endoderm for head formation in the mouse. *Development* **126**, 4925-4932.
- Simeone, A., Acampora, D., Mallamaci, A., Stornaiuolo, A., D'Apice, M. R., Nigro, V. and Boncinelli, E. (1993). A vertebrate gene related to orthodenticle contains a homeodomain of the Bicoid class and demarcates anterior neuroectoderm in the gastrulating mouse embryo. *EMBO J.* **12**, 2735-2747.
- Taira, M., Otani, H., Saint-Jeannet, J. P. and Dawid, I. B. (1994). Role of the LIM class homeodomain protein Xlim-1 in neural and muscle induction by the Spemann organizer in *Xenopus*. *Nature* **372**, 677-679.
- Takada, S., Stark, K. L., Shea, M. J., Vassileva, G., McMahon, J. A. and McMahon, A. P. (1994). Wnt-3a regulates somite and tailbud formation in the mouse embryo. *Genes Dev.* **8**, 174-189.
- Tam, P. P. and Zhou, S. X. (1996). The allocation of epiblast cells to ectodermal and germ-line lineages is influenced by the position of the cells in the gastrulating mouse embryo. *Dev. Biol.* **178**, 124-132.
- Tam, P. P. and Steiner, K. A. (1999). Anterior patterning by synergistic activity of the early gastrula organizer and the anterior germ layer tissues of the mouse embryo. *Development* **126**, 5171-5179.
- Thomas, P. and Beddington, R. (1996). Anterior primitive endoderm may be responsible for patterning the anterior neural plate in the mouse embryo. *Curr. Biol.* **6**, 1487-1496.
- Torigoi, E., Bennani-Baiti, I. M., Rosen, C., Gonzalez, K., Morcillo, P., Ptashne, M. and Dorsett, D. (2000). Chip interacts with diverse homeodomain proteins and potentiates bicoid activity in vivo. *Proc. Natl. Acad. Sci. USA* **97**, 2686-2691.
- Tsang, T. E., Shawlot, W., Kinder, S. J., Kobayashi, A., Kwan, K. M., Schughart, K., Kania, A., Jessell, T. M., Behringer, R. R. and Tam, P. P. (2000). Lim1 activity is required for intermediate mesoderm differentiation in the mouse embryo. *Dev. Biol.* **223**, 77-90.
- Tsang, T. E., Khoo, P. L., Jamieson, R. V., Zhou, S. X., Ang, S. L., Behringer, R. and Tam, P. P. (2001). The allocation and differentiation of mouse primordial germ cells. *Int. J. Dev. Biol.* **45**, 549-555.
- Varlet, I., Collignon, J. and Robertson, E. J. (1997). Nodal expression in the primitive endoderm is required for specification of the anterior axis during mouse gastrulation. *Development* **124**, 1033-1044.
- Visvader, J. E., Mao, X., Fujiwara, Y., Halm, K. and Orkin, S. H. (1997). The LIM-domain binding protein Ldb1 and its partner LMO2 act as negative regulators of erythroid differentiation. *Proc. Natl. Acad. Sci. USA* **94**, 13707-13712.
- Wadman, I. A., Osada, H., Grutz, G., Agulnick, A. D., Westphal, H., Forster, A. and Rabbitts, T. H. (1997). The LIM-only protein Lmo2 is a bridging molecule assembling an erythroid, DNA-binding complex which includes the TAL1, E47, GATA-1 and Ldb1/NLI proteins. *EMBO J.* **16**, 3145-3157.
- Wang, S., Krinks, M., Lin, K., Luyten, F. P. and Moos, M. (1997). Frzb, a secreted protein expressed in the Spemann organizer, binds and inhibits Wnt-8. *Cell* **88**, 757-766.
- Weinstein, D. C., Ruiz Altaba, A., Chen, W. S., Hoodless, P., Prezioso, V. R., Jessell, T. M. and Darnell, J. E., Jr (1994). The winged-helix transcription factor HNF-3 beta is required for notochord development in the mouse embryo. *Cell* **78**, 575-588.
- Winnier, G., Blessing, M., Labosky, P. A. and Hogan, B. L. (1995). Bone morphogenetic protein-4 is required for mesoderm formation and patterning in the mouse. *Genes Dev.* **9**, 2105-2116.
- Ying, Y., Liu, X. M., Marble, A., Lawson, K. A. and Zhao, G. Q. (2000). Requirement of Bmp8b for the generation of primordial germ cells in the mouse. *Mol. Endocrinol.* **14**, 1053-1063.
- Yamaguchi, T. P. (2001). Heads or tails: Wnts and anterior-posterior patterning. *Curr. Biol.* **11**, R713-R724.
- Yamashita, T., Agulnick, A. D., Copeland, N. G., Gilbert, D. J., Jenkins, N. A. and Westphal, H. (1998). Genomic structure and chromosomal localization of the mouse LIM domain-binding protein 1 gene, Ldb1. *Genomics* **48**, 87-92.
- Zeng, L., Fagotto, F., Zhang, T., Hsu, W., Vasicsek, T. J., Perry, W. L. 3rd, Lee, J. J., Tilghman, S. M., Gumbiner, B. M. and Costantini, F. (1997). The mouse Fused locus encodes Axin, an inhibitor of the Wnt signaling pathway that regulates embryonic axis formation. *Cell* **90**, 181-192.